Analyzing Concrete Cracking Along Civil Infrastructure using Distributed Fiber Optic Sensing

CHRISTOPH M. MONSBERGER, MADELEINE WINKLER, ROMAN PAVELKIN, LUIS ZAVALA MONDRAGON, FONS VAN DER SOMMEN, ANNA THERESA KORNBERGER, DIRK SCHLICKE and WERNER LIENHART

ABSTRACT

Crack monitoring using distributed fiber optic sensing (DFOS) in civil engineering has evolved significantly during recent years. Scientific and commercial applications often focus on distributed strain sensing based on Rayleigh scattering due to its high spatial and strain resolution despite its limited sensing range. Brillouin sensing techniques are more suitable for monitoring large-scale civil infrastructure as they can provide measurements over numerous kilometers. The improved sensing range, however, results in spatial limitations and therefore, restricted suitability for strain-based crack monitoring.

This paper presents an enhanced laboratory test series, in which the suitability of various Brillouin interrogators for concrete crack monitoring was evaluated. Five individual concrete specimens equipped with multiple installation setups were investigated under well-known laboratory conditions, where the resulting fiber optic strain sensing data could be related to the true crack width obtained by high-resolution distance transducers over the crack. An alternative method relates alterations in the raw Brillouin frequency spectrum (BFS) to local distortion events like cracks, which is however an extensive, time-consuming process. Artificial intelligence (AI) is therefore applied to the test data to identify BFS anomalies and relate them to the locally arising crack width. First results demonstrate that AI can be an efficient tool to optimize traditional DFOS monitoring strategies, but further optimization is required for reliable determination.

INTRODUCTION

Cracks inside concrete structures, i.e. their width and temporal alteration, are key indicators for civil infrastructure assessment as they usually correlate with changes in loading condition and imposed deformation. Comprehensive documentation of existing and emerging cracks is therefore essential and is usually provided manually within bridge or tunnel inspections using manual crack meters. Conventional automated sys-

C. M. Monsberger, M. Winkler, ACI Monitoring GmbH, 8010 Graz, Austria
R. Pavelkin, L. Z. Mondragon, F. v.d. Sommen, Eindhoven University of Technology, 5612 AP Eindhoven, Netherlands
A. T. Kornberger, Konig und Heunisch Planungsgesellschaft mbH, 04109 Leipzig, Germany
D. Schlicke, W. Lienhart, Graz University of Technology, 8010 Graz, Austria

tems are often either limited in their spatial resolution by providing discrete points only or require a visual line-of-sight on the surface.

Distributed fiber optic sensing (DFOS) is extensively used for concrete crack monitoring in recent years, especially in scientific-related projects and laboratory testing. These applications mainly focus on Rayleigh scattering due to its high spatial resolution and strain resolution (e.g. [1] or [2]), but with significant restrictions in the sensing range. Brillouin sensing techniques are more suitable for monitoring large-scale civil infrastructure as they can provide measurements over numerous kilometers, which however results in spatial limitations and therefore impedes the capabilities for strain-based crack monitoring. An alternative method relates alterations (c.f. double peaks) in the raw Brillouin frequency spectrum (BFS) to arising local cracking (see e.g. [3]). Any manual assessment and classification of the Brillouin spectrum is however an extensive, time-consuming process due to the comprehensive data amount along large civil infrastructures, which suggests more sophisticated approaches based on machine learning techniques and Artificial Intelligence (AI).

This contribution reports about a dedicated laboratory test series, in which the suitability of various Brillouin interrogators for identifying and quantifying concrete cracks has been investigated. In the following, the monitoring setup including five individual test concrete specimens equipped with multiple installation setups as well as the crack determination algorithm based on numerical integration is introduced. Derivations from various Brillouin sensing interrogators are presented and compared to Rayleigh sensing data as well as the true reference crack width obtained by traditional, high-resolution distance transducers. The obtained Brillouin sensing data is also examined by AI-based methods to identify BFS anomalies and relate them to the locally arising crack width. Finally, an outlook on future research is given.

LABORATORY TEST SETUP AND CRACK SENSING ALGORITHM

In order to implement comprehensive data for strain-based crack assessment as well as for AI evaluation, an enhanced test series consisting of five concrete test specimens was carried out at Graz University of Technology (TU Graz, Laboratory for Structural Engineering). All individual specimens feature a squared cross-sectional profile with a width and height of 200 mm, and a total specimen length of 3000 mm as schematically shown in Figure 1 (left). Each test structure was equipped with one central reinforcement bar (diameter: 18 mm) for applying the loading force during testing. In addition, thin steel plates were installed before concreting to weaken the cross-section at defined locations, which ensures a controlled cracking of the structure during loading. The five specimens vary depending on the number of crack locations, with different configurations from one to five cracks being realized.

The testing specimens were equipped with multiple layers of fiber optic sensing cables, including tight-buffered optical fibers [4] as well as prefabricated sensing cables from numerous manufacturers [5–7]. The sensors were glued to the reinforcement, directly embedded inside the specimens in different arrangement and also glued to the outer surface using different adhesive after concreting (Figure 1, middle). Each specimen was tested separately under controlled axial loading, where the rebar was fixed at

the bottom and pulled apart at the top side (Figure 1, right) to initialize the crack opening along the structure at the predefined locations. Loading was performed step-wise up to loads of 180 kN (depending on the specimen), where the DFOS installation was subsequently monitored with all different interrogators at each loading step.

DFOS basically delivers distributed strain (and temperature) profiles along the longitudinal axis of the installed optical sensing fiber. Discrete cracking is usually reproduced as local strain peak (c.f. Figure 2) in the DFOS signal. To relate the obtained information to the crack width itself, the strain values can be numerically integrated over the area of interest, in which the crack appears along the structure. This integration length, or rather its start and end point along the signal, can be practically determined by analyzing the strain gradient at each side of the peak. Hence, the strain difference from point j to j+1 is calculated in relation to the difference to the maximum peak (Figure 2). The start or end point is identified as the location, at which the ratio does not exceed a specified threshold

Figure 1. Laboratory test setup: Schematic representation (left), manufactured test specimens with applied DFOS cable (middle) and practical realization with one crack definition (right).

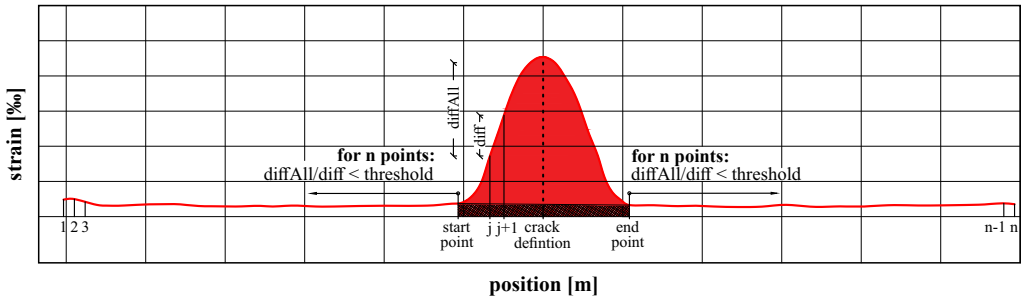

Figure 2. Schematic representation of arising crack in DFOS signal and integration length for crack width derivation (based on [8]).

over a defined number of following data points. For further information and details on the determination principle reference is given to [8].

STRAIN-BASED CRACK ANALYSIS AND RESULTS

The five sample test series aim to analyze crack patterns with different spacing and crack widths. Loading for all specimens was performed in two steps with 15 kN each up to the initial cracking, which was determined to be around 30 kN. Afterwards, the load was further increased in 10 kN steps up until the ultimate failure of the structure at around 100 kN and beyond. By applying the mechanical crack initiation steel plates, it could be ensured that major cracks only open at well defined locations. The strain-based sensing results presented in this paper focus on a specimen with one crack location.

DFOS measurements were performed by Brillouin interrogators from three different manufacturers utilizing the Brillouin Optical Time Domain Analysis (BOTDA) as well as the the Brillouin Optical Frequency Domain Analysis (BOFDA) with a spatial resolution of 0.5 m. Reference measurements were taken using a high-resolution OBR from Luna Innovations Inc. (USA) based on the OFDR (Optical Frequency Domain Reflectometry) to verify the obtained strain profiles. In addition, multiple distance transducers (DD-1) from HBM GmbH (Germany) were placed at the specimens' surface to monitor the crack opening and corresponding width.

The resulting strain sensing profiles of one selected sensing cable for all different DFOS interrogators are depicted in Figure 3). It must be noted that the data represents the raw measurement signal and is not further processed or filtered. The high-resolution OFDR measurements (left) confirms the crack opening at 30 kN, with a significant peak arising in the middle of the specimen (position: 1.5 m) over an area of approx. 200 mm.

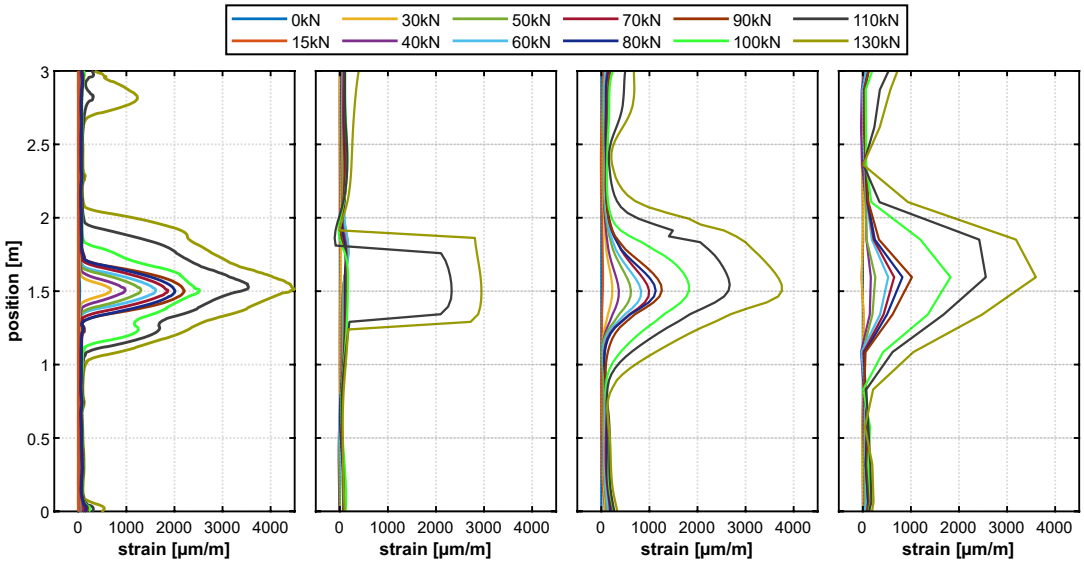

Figure 3. Strain profiles recorded by various DFOS interrogators during load test: Rayleigh OFDR and Brillouin B-01/B-02/B-03 (left to right).

TABLE I. CRACK WIDTHS DETERMINED FROM DFOS AND MEASURED BY CONVENTIONAL DISTANCE TRANSDUCERS AT DIFFERENT LOAD LEVELS

load [kN]	crack width [mm]				
	DD-1	**OFDR**	**B-01**	**B-02**	**B-03**
15	0.00	0.00	0.00	0.00	0.00
30	0.14	0.06	0.08	0.08	0.00
40	0.20	0.11	0.15	0.13	0.14
50	0.28	0.24	0.24	0.24	0.23
60	0.35	0.32	0.31	0.29	0.31
70	0.42	0.39	0.36	0.36	0.39
80	0.51	0.47	0.46	0.39	0.47
90	0.60	0.57	0.57	0.45	0.72
100	0.89	1.01	1.11	0.89	1.21
110	1.23	1.57	1.76	1.52	1.94
130	1.62	2.56	2.64	2.39	3.04

The Brillouin sensing techniques can not capture the initial cracking with such high resolution due to their spatial limitations, even if interrogator B-02 also indicates cracking already at 30 kN. With increasing load, the peak width and magnitude is continuously increasing up to the maximum load of 130 kN applied for the actual specimen. Although the strain peak appears over a larger area, the Brillouin interrogators can represent the OFDR technique well for loads higher than 30 kN expect for B-01, which only indicates major strain events for the last two load steps. Comprehensive data reprocessing using the full Brillouin spectrum however significantly optimizes the data representation for this interrogator and can enable crack derivation in a reliable manner. The comparison between the raw and optimized data is further discussed in [9].

By determining the integration length and numerical integration, the effective crack width can be evaluated at the crack location. The numerical values are listed in Table I for all DFOS technologies and the reference distance transducer. The determined crack widths show good agreement between the high-resolution OFDR and the Brillouin sensing systems, with maximum deviations lower than 0.1 mm at loads of up to 80 kN or rather a width of approx. 0.5 mm. Structure-relevant concrete cracks are usually defined in civil engineering with 0.3 mm and higher. This critical range can be unambiguously derived for all sensors. Absolute accuracy is confirmed by the distance transducers on the surface up to 90 kN. Higher loads indicates the ultimate failing progress of the structure, which is why the crack width derivation using numerical strain integration is no longer applicable.

It must be noted that the quality of the crack width derivation is strongly related to the parameter settings for the integration length. These vary depending on not only the sensing technique but also the installation technique of the optical sensing cable. The dedicated test series is capable of providing an essential lookup table to appropriately perform the integration length determination for different configurations for future monitoring applications.

ARTIFICIAL INTELLIGENCE: METHODOLOGY AND RESULTS

The assessment and classification of strain-based DFOS data is usually done by manual routines and is therefore an extensive, time-consuming process due to the comprehensive data amount the monitored structure, which implies optimized techniques based on Artificial Intelligence. This section demonstrates the general capabilities and potential of combining BOFDA data with AI technologies for crack identification and quantification in civil structural health monitoring.

Conventional Brillouin sensing techniques evaluate strain by determining changes of the mean Brillouin frequency shift (BFS), which often rely on single-peak curve fitting by Lorentzian models. Brillouin sensing systems might be however restricted for crack identification with small width due to their limitations in the spatial resolution. It could be already shown that double peaks can arise in the Brillouin spectrum if local stress events like cracks occur (c.f. [3]). Nevertheless, signals from practical applications might diverge from the anticipated Lorentzian profile [10], which is why machine learning becomes necessary to address more complex BFS patterns (e.g. [11]).

Training Details and AI Model

The approach followed in this paper aims to automate two tasks with machine learning algorithms. The automation identifies anomalous BFS spectra along the optical network and a regression approach to estimate the crack width. Both automations are based on the similar approach for multiclass DFOS event classification reported in [12], but consists of two main stages as schematically shown in Figure 4. The first stage is an extraction of spectral features using a pre-trained 1D-CNN (Convolutional Neural Network) autoencoder [13]. The reason for choosing this model is that autoencoders can learn noise-robust latent representations by extracting only essential features while removing irrelevant variations. The entire model contains approx. 185,000 trainable parameters, where training was performed to remove noise from both, normal and anomalous BFS data for 50 epochs.

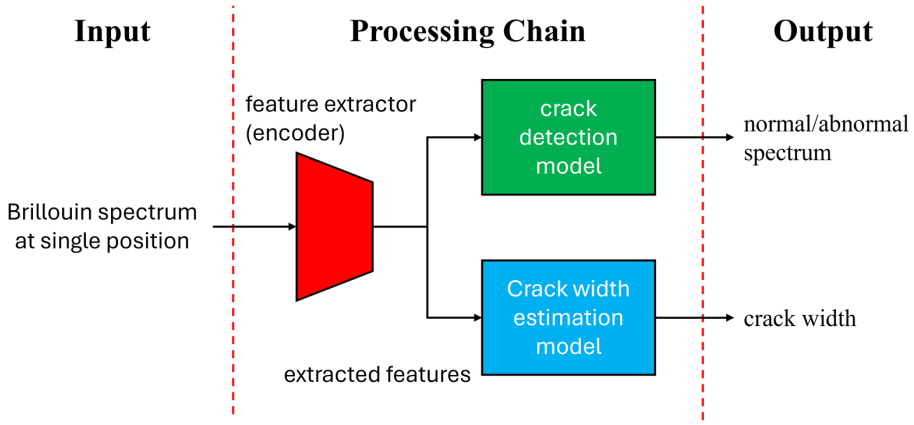

Figure 4. Schematic workflow of AI model including feature extractor (encoder) and decision tree ensembles.

The second stage of AI model uses two ensembles of decision trees that are trained with the Extreme Gradient Boosting machine (XGBoost) [14] on the features extracted at the first stage. The first ensemble is trained for binary classification (AD) implemented within the optimization framework Optuna [15]. Optuna is a robust hyperparameter optimization framework using a Tree-structured Parzen Estimator, enabling informed decision-making, early stopping, making it an essential tool for complex tasks. The model output is a binary decision whether the signal is anomalous or not. In addition, a regression model is trained in the second step to quantify crack widths, optimizing the reduction of the Root Mean Squared Error (RMSE).

This combined architecture was chosen as it balances CNN performance for feature extraction and robustness of XGBoost machines for overfitting on small datasets of limited diversity, which can limit AI models for monitoring applications in civil engineering.

Training Dataset and First Results

To train, validate and test the ML model, the data of four different concrete specimens of the test series is utilized. The crack location is manually labeled for each loading step. The Brillouin spectra of the first three specimens is used for training and validation of the ML models, encompassing approx. 57,000 BFS samples. Model testing is performed based on the data of the fourth specimen. The crack width dataset is less comprehensive as only approx. 1,600 anomalous BFS samples represent crack locations referenced with conventional measurements.

The AD XGBoost model was evaluated by calculating accuracy (= 0.8545), precision (= 0.7575), recall (= 0.6492), and F1-score (= 0.6992). The corresponding confusion matrix for the model testing is depicted in Figure 5 (left). It can be seen that the model

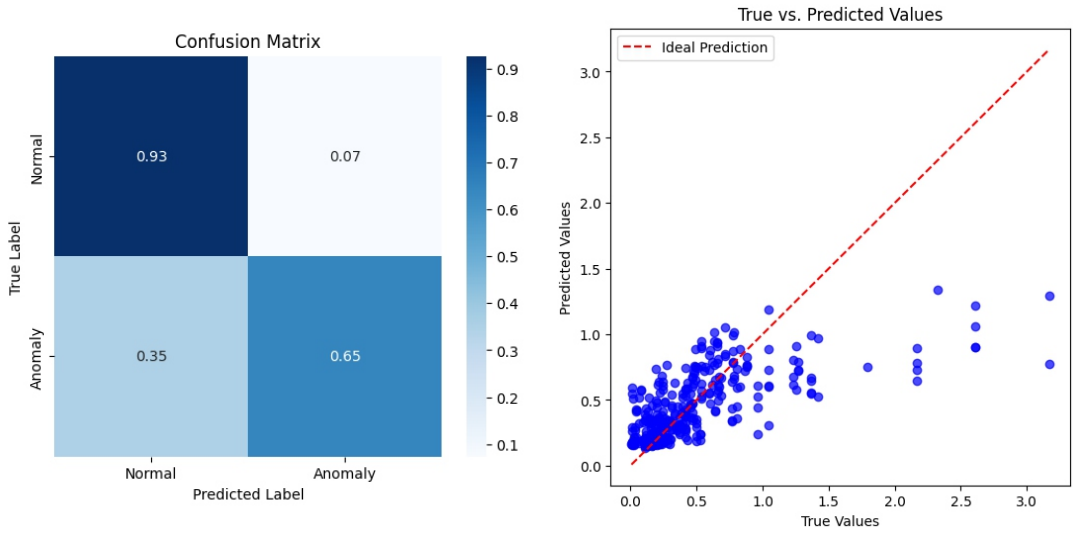

Figure 5. AI modeling results: Confusion matrix (normalized row-wise) plotted after passing the test set through the AD XGBoost classifier (left) and regression plot for true vs. predicted values of crack width through XGBoost regressor (right).

is capable to distinguish normal BFS (true negatives) quite well and outputs low number of false positives. However, a significant portion of anomalies is labeled as normal BFS (35 % of false negatives), resulting in a low overall F1-score. This could potentially result from the typical similarity of the overall BFS data to normal BFS data.

The output of the XGBoost regressor model can be presented as the relation between the predicted values of the crack width and the true reference values as shown in Figure 5 (right). It can be noted that the regression does not fit well for numerous predicted crack widths, where the average RMSE must be indicated with 0.3799 mm. The coefficient of determination, R^2, showing is the proportion of the variation in the dependent variable that is predictable from the independent variable, is equal to 0.4240, proving the significant spread in the predicted values.

CONCLUSIONS AND OUTLOOK

In this paper, two different methods were implemented to analyze crack widths along reinforced concrete structures using distributed fiber optic sensors based on Brillouin sensing. An enhanced test series with five individual specimens equipped with multiple DFOS installation setups was realized to investigate crack opening under well-known laboratory conditions. The resulting strain profiles could be numerically integrated to obtain crack widths at the crack locations for different load levels. The derived values correspond well with reference measurements from distance transducers mounted at the surface for all tested Brillouin interrogators, with maximum deviations lower than 0.1 mm before the ultimate failure progress of the specimen.

In addition, AI-based evaluation was applied to the raw Brillouin frequency spectrum to identify local distortion events like cracks and derive corresponding widths. Although first tests could show that AI is capable to classify normal spectrum behavior well, further optimization is required for anomalous spectra to avoid misclassifications. Furthermore, the regression model to derive numerical crack widths needs significant improvement for reliable derivation.

The realized test series provides a wide range of Brillouin sensing data measured by different interrogators along multiple sensing cable inside concrete structures. Up to now, there is no distinction between cable type or installation technique within the AI model. The evaluation strategy will be optimized by including corresponding information or rather by selecting more suitable installation techniques for model training. Moreover, it might be useful to combine local deficiency identification using AI models with conventional strain-based analysis to determine crack widths more reliably.

ACKNOWLEDGMENT

The laboratory test series and the monitoring program was carried out within the collective research project “AI FORSchung” (Nr. 52106504) financed by the Austrian Research Promotion Agency (FFG), which is part of the EUREKA Clusters AI Call 2021.

REFERENCES

1. Richter, B., M. Herbers, and S. Marx. 2024. “Crack monitoring on concrete structures with distributed fiber optic sensors–Toward automated data evaluation and assessment,” *Structural Concrete*, 25(2):1465–1480, doi:10.1002/suco.202300100.
2. Vorwagner, A., M. Kwapisz, W. Lienhart, M. Winkler, C. Monsberger, and D. Prammer. 2021. “Verteilte Rissbreitenmessung im Betonbau mittels faseroptischer Sensorik – Neue Anwendung von verteilten faseroptischen Messsystemen,” *Beton- und Stahlbetonbau*, 116(10):727–740, doi:10.1002/best.202100060.
3. Ou, R., L. Luo, and K. Soga. 2022. “Brillouin scattering spectrum-based crack measurement using distributed fiber optic sensing,” *Structural Health Monitoring*, 21(4):1345–1366, doi:10.1177/14759217211030913.
4. TLC. 2020. *Data Sheet: Tight Buffer*, Rev. 3.0 11/12/2020, The Light Connection Inc.
5. Solifos. 2019. *BRUsens DSS 3.2mm V9 grip 3_50_2_005*, Solifos AG.
6. SHM. 2025. *EpsilonSensor*, SHM Systems Company.
7. sucess4u GmbH. 2023. *FIBRASENS DSS 2f*, Datasheet Fiber Optic Cable DS220801D.
8. Kornberger, A. T. 2024. *Dehnungsvergleiche von FE basierten Analysen und Faseroptikmessungen an Zugversuchen*, Master’s thesis, Graz University of Technology, Graz, Austria.
9. Monsberger, C., M. Winkler, A.-T. Kornberger, and D. Schlicke. 2025. “Identification and quantification of concrete cracks using various distributed fiber optic sensing techniques,” in *13th International Conference on Structural Health Monitoring of Intelligent Infrastructure (SHMII-13)*, Society for Civil Structural Health Monitoring (SCSHM), Verlag der Technischen Universität Graz.
10. Karapanagiotis, C. and K. Krebber. 2023. “Machine learning approaches in Brillouin distributed fiber optic sensors,” *Sensors*, 23(13):6187, ISSN 1424-8220, publisher: MDPI.
11. Wang, B., L. Wang, N. Guo, Z. Zhao, C. Yu, and C. Lu. 2019. “Deep neural networks assisted BOTDA for simultaneous temperature and strain measurement with enhanced accuracy,” *Optics express*, 27(3):2530–2543, ISSN 1094-4087, publisher: Optical Society of America.
12. Wu, H., J. Chen, X. Liu, Y. Xiao, M. Wang, Y. Zheng, and Y. Rao. 2019. “One-dimensional CNN-based intelligent recognition of vibrations in pipeline monitoring with DAS,” *Journal of Lightwave Technology*, 37(17):4359–4366, ISSN 0733-8724, publisher: OSA.
13. Gondara, L. 2016. “Medical image denoising using convolutional denoising autoencoders,” IEEE, ISBN 1-5090-5910-5, pp. 241–246.
14. Chen, T. and C. Guestrin. 2016. “Xgboost: A scalable tree boosting system,” pp. 785–794.
15. Akiba, T., S. Sano, T. Yanase, T. Ohta, and M. Koyama. 2019. “Optuna: A next-generation hyperparameter optimization framework,” pp. 2623–2631.